Received: 7 September 2024 | Revised: 22 December 2024 | Accepted: 3 February 2025

DOI: 10.1111/epi.18320

Epilepsia

RESEARCH ARTICLE

Prognostic application of lesion network mapping to epilepsy surgery outcomes in pediatric tuberous sclerosis complex

Kara B. Miecznikowski[1] | **Hansel M. Greiner**[2,3] | **James Leach**[4,5] | **Leonid Rozhkov**[2] | **Francesco T. Mangano**[6,7] | **Darcy A. Krueger**[2,3] | **Mark W. DiFrancesco**[4,5]

[1]University of Cincinnati College of Medicine, Cincinnati, Ohio, USA

[2]Division of Neurology, Cincinnati Children's Hospital Medical Center, Cincinnati, Ohio, USA

[3]Department of Pediatrics, Division of Neurology, University of Cincinnati College of Medicine, Cincinnati, Ohio, USA

[4]Department of Radiology, Cincinnati Children's Hospital Medical Center, Cincinnati, Ohio, USA

[5]Department of Radiology, University of Cincinnati College of Medicine, Cincinnati, Ohio, USA

[6]Division of Neurosurgery, Cincinnati Children's Hospital Medical Center, Cincinnati, Ohio, USA

[7]Department of Neurosurgery, University of Cincinnati College of Medicine, Cincinnati, Ohio, USA

Correspondence
Mark W. DiFrancesco, Department of Radiology, University of Cincinnati College of Medicine, Cincinnati, OH, USA.
Email: mark.difrancesco@cchmc.org

Abstract

Objective: Patients with tuberous sclerosis complex (TSC)-related epilepsy often have drug-refractory epilepsy and numerous potential epileptogenic tubers. Current clinical methods target tubers for resection, but prediction of resulting seizure relief is difficult. This study describes implementation of lesion network mapping in TSC patients undergoing epilepsy surgery to associate resection zone with seizure outcomes.

Methods: Thirty-nine consecutive patients with TSC who underwent invasive electroencephalography (EEG) and resection or ablation of the seizure onset zone were included. After preprocessing, each resection zone was delineated as the region of interest. Lesion network mapping was performed to determine the association between cortical networks connected to the resection zone and postoperative outcome using a multiple regression, iterative model that included demographic and other variables obtained from analysis of invasive EEG.

Results: Of 39 patients, 20 (51%) had a good International League Against Epilepsy outcome (1–3). Resection regions connected to the default mode network and motor network were associated with better seizure outcome. Regions connected to the bilateral insula, visual associative regions, and putamen were associated with poor seizure outcome.

Significance: This study provides methodology for lesion network mapping in TSC-related epilepsy. The results suggest a tendency for better outcomes when the resection zone is connected to certain networks, including the default mode and motor networks, that may support sustainment of seizures.

KEYWORDS

default mode network, epilepsy surgery, functional connectivity, lesion network mapping, tuberous sclerosis complex

1 | INTRODUCTION

Tuberous sclerosis complex (TSC) is a genetic disorder in which primarily benign tumors develop in various organ systems across the body.[1,2] In the brain, cortical tubers and related histopathological changes result in recurrent seizures in up to 90% of TSC patients,[3] with approximately 50% of patients developing drug-refractory epilepsy.[4] Epilepsy that fails to improve with antiepileptic drugs can be addressed with surgical treatment, which aims to remove or disconnect seizure-generating areas of the brain, referred to as the seizure onset zones (SOZs). Seizure freedom has been demonstrated at 1-year follow up in 50%–60% of TSC patients following epilepsy surgery,[5,6] with an additional 18%–34% having significant reduction in seizure frequency.[7,8]

Neuronal activation in a region of the brain is followed by a hemodynamic response in which cerebral blood flow and oxygen supply to the area are increased.[9] Functional magnetic resonance imaging (fMRI) uses the difference in magnetic susceptibility between oxygenated and deoxygenated blood to measure a blood oxygenation level-dependent (BOLD) signal corresponding to neuronal activity stimulated by a task. At rest and during sustained periods of a task, the BOLD signal fluctuates spontaneously at low frequencies (<.1 Hz) in different regions of the brain.[10] Synchronous fluctuations in BOLD signal between spatially distinct areas of the brain represent a functional connectivity between these regions; canonical networks of functional connectivity have been established at rest that correspond with neuronal activation patterns elicited by cognitive, language, and motor tasks. Prominent among the resting-state functional networks is the default mode network (DMN),[11] comprised partly of medial frontal and posterior regions and lateral parietal regions, that is tonically active during rest and deactivated during active tasks. Resting-state fMRI (rs-fMRI) has been used to assess the brain's functional architecture in both healthy individuals and patients with a wide variety of neurologic and psychiatric disorders.[12]

The technique of lesion–symptom mapping attempts to associate lesion location with outcomes by determining the spatial overlap of lesions from patients who experience similar outcomes. In cohorts of patients with TSC or other focal cortical dysplasia (FCD), this approach can be challenging, as lesions may rarely overlap. Lesion network mapping (LNM) is a recently developed alternative approach that accounts for involvement of a lesioned region in brain networks. LNM maps how a lesioned region would be functionally connected in healthy brains and compares those maps among patients with different outcomes to determine whether certain patterns of connectivity predict outcome. In a study of patients with FCD who underwent surgery for refractory epilepsy, Bdaiwi et al. found that lesions more strongly anticorrelated to the DMN were less likely to result in seizure freedom following resection, implying that the lesion's disruption of network connectivity, rather than simply the functionality of the region in which it lies, may affect surgical outcomes.[13] Similarly, a study of patients with various seizure etiologies using LNM found that lesion ablations that did not result in seizure freedom were preferentially located in regions connected to several canonical resting-state networks[14]; these were more than twice as likely to be functionally connected to the DMN, language network, and visuospatial network.[15] Notably, there was no significant correlation between anatomical location of ablation and seizure outcome.

Key points

- Lesion network mapping was used to determine association between network connectivity and outcomes following pediatric TSC epilepsy surgery.
- Good outcomes were observed in 51% of cases.
- Connectivity of resected seizure onset zone and surrounding tissue to certain networks such as the default mode and motor networks was associated with better outcome.
- This study provides methodology for lesion network mapping in TSC-related epilepsy.

Although some studies have used connectivity analyses to plan for eloquent tissue conservation in neurosurgery and correlate functional network connectivity with other factors such as neurodevelopmental state and tuber burden in TSC patients, to our knowledge none has used functional connectivity to predict surgical outcomes. The present study aimed to correlate functional connectivity and surgical outcomes in TSC patients undergoing epilepsy surgery using rs-fMRI data from matched healthy controls. Based on our prior work, we hypothesized that lesions occupying regions negatively correlated to the DMN in healthy brains would be associated with poorer outcomes in TSC patients undergoing epilepsy surgery.[16]

2 | MATERIALS AND METHODS

2.1 | Patient cohort

This retrospective study included 39 TSC patients (23 male, 16 female) who underwent resective epilepsy surgery with 1-year follow-up. Median age was 48 months (range = 12–394 months, interquartile range = 30–135 months). Patient data were collected over the 14-year period of 2007 to 2021. Preoperative electroencephalographic (EEG) data were acquired with either subdural grid or depth electrodes to determine the SOZ region for each patient. Retrospectively, the intracranial EEG (iEEG) data were reviewed by a single epileptologist (H.M.G.) blinded to the clinical report, ultimate surgery recommended, and seizure outcome. At our institution, over the period of data collection, there was a shift from subdural electrode monitoring (2007–2015) to predominantly stereo-EEG (sEEG) monitoring (2016–current). A variety of electrode manufacturers and techniques were used. However, all iEEG tracings were recorded at 2-kHz digitation rate using either silastic subdural grids with platinum contacts spaced 10 mm from center to center, or sEEG electrodes with contacts spaced 2.5–10 mm. Each patient chart was reviewed to determine number of clinical seizure types. The iEEG tracings for a minimum of two examples for each seizure type were reviewed in both standard band pass filter (1–100 Hz) and "open" high-pass filter (>1 Hz) settings, in both average reference and bipolar montages. SOZ was defined as the group of contacts that demonstrated the earliest sustained ictal change and similar ictal frequency and morphology. If there were significant differences between seizures reviewed, both contact groups were included in the SOZ. This process was repeated for each seizure type. If the group of contacts comprising the SOZ was different between seizure types, these were defined as separate SOZs. Extent of SOZ was defined by number of unique SOZ contacts present, considering all SOZs equally. Ictal patterns were categorized as either rhythmic spiking, defined as low-frequency rhythmic spikes as the predominant ictal pattern, or high-frequency oscillations, defined as low-amplitude, high-frequency (>80 Hz) activity identified at seizure onset. Surgical outcome at minimum 1-year follow-up was recorded as a standardized International League Against Epilepsy (ILAE) score, ranging from 1 (seizure-free) to 6 (>100% increase in baseline seizure days).[17]

2.2 | Delineation of SOZ resection regions

Pre- and postoperative clinical neuroimaging, supplemented by examination of intraoperative photographs and three-dimensional reconstruction of electrodes coregistered to the patient's postoperative computed tomography using Analyze software package 14.0 (AnalyzeDirect), allowed delineation of the extent of SOZ resection for each patient. Preoperative and postoperative brain MRI was performed utilizing variable techniques, with all examinations including volumetric pre- and postcontrast T1 volumetric images (1 mm isotropic), T2-weighted, and T2 fluid-attenuated inversion recovery sequences. The postoperative study with the best imaging quality and best definition of the resection region was utilized to assess resection volume. Pre- and postoperative images were fused utilizing BrainLab iPlan 3.0. Resection regions were traced on each image and modified as necessary for resection cavity retraction and shift using gyral–sulcal landmarks referencing postoperative images of the operative field during resection. Burnt-in-pixel images of the resection volume overlayed on preoperative volumetric T1-weighted images were then imported into MRIcron (version 1, 2015, https://www.nitrc.org/projects/mricron). This procedure resulted in a three-dimensional region of interest (ROI) mask corresponding to the resected tissue for each patient.

2.3 | Lesion network mapping

This study represented the functional connectivity profile of each resection ROI by calculating the mean seed-to-voxel connectivity map, using the ROI as seed, among rs-fMRI data from healthy individuals. Cincinnati MR Imaging of Neuro-Development (C-MIND; https://research.cchmc.org/c-mind/manual-project-overview), an imaging database of healthy children collected at our institution under National Institutes of Health contract HHSN275200900018C,[18] provided 200 datasets from 129 individuals evenly distributed in age at acquisition from 2.9 to 18.9 years (86 male, 43 female). Each dataset included a T1-weighted high-resolution structural volume (1 mm isotropic) and an rs-fMRI series of 150 volumes acquired without sedation and while the subject was awake (echo-planar sequence covering the whole brain with repetition time = 2000 ms, echo time = 35 ms, $3 \times 3 \times 4$ mm voxel size). Our prior publication[13] provides more details about the C-MIND data.

Preprocessing of the C-MIND data followed standard protocol in Statistical Parametric Mapping software (SPM12; http://www.fil.ion.ucl.ac.uk/spm/software/spm12/) in the MATLAB computing environment (MathWorks). This included realignment of the rs-fMRI series, coregistration of the T1-weighted volume to the mean realigned rs-fMRI volume, unified tissue segmentation and normalization[19] of the T1-weighted volume subsequently applied to the rs-fMRI series, and smoothing using an 8-mm Gaussian kernel. This same preprocessing protocol, starting with T1-weighted volumes and resection ROI delineated for each TSC patient, resulted in corresponding spatially normalized representations of each resection mask.

The CONN Toolbox v22a (https://www.nitrc.org/projects/conn),[20] with normalized preprocessed C-MIND data

TABLE 1 Tuberous sclerosis complex patient characteristics ($N=39$).

Characteristic	Median	Interquartile range	Minimum	Maximum
Age at resection, months	48	30–135	12	394
SOZ electrode contacts, *n*	7	4–12	2	25
Resection volume, cm^2	45.6	17.1–78.1	1.5	164.7
Sex, *n*	25 male / 14 female			
Ictal pattern, *n*	12 rhythmic spiking/11 HFO/16 both			
ILAE class at 1-year follow-up, classes 1–6, *n*	14, 3, 3, 9, 10, 0			

Abbreviations: HFO, high-frequency oscillations; ILAE, International League Against Epilepsy; SOZ, seizure onset zone.

as input, was used to calculate for each TSC patient the mean seed-to-voxel connectivity map, using the patient's resection ROI as seed, among the 15 C-MIND rs-fMRI datasets closest in age and with the same gender as the TSC patient. Connectivity maps were generated at resolution of 2 mm isotropic. The large size of many of the resection ROIs (interquartile size range = 17.1–78.1 cm^2; see Table 1), however, prompted concern of losing spatial specificity when averaging the rs-fMRI signal for seed-to-voxel connectivity calculations. Our processing pipeline mitigated this concern by using instead the first principal component of the resection ROI signal.

2.4 | Statistical analysis

We applied multiple regression in SPM12 voxelwise to the mean C-MIND connectivity maps corresponding to the resection ROI for the patients. The model explained the connectivity to each voxel among the patients (as dependent variable) as a function of the ILAE score at 1-year follow-up, with age, sex, ictal pattern, and number of SOZ electrode contacts used as covariates. Assessment of the dependence of connectivity on ILAE score at 1-year follow-up after resection began by application of a nominal voxel threshold of $p < .001$ to the ILAE score model coefficient. Clusters of voxels above this threshold reaching a clusterwise threshold of $p < .05$ after familywise error correction for multiple comparisons were considered statistically significant.

Consideration of our limited sample size and acknowledgement of subsequent type II errors led us to also express our model results in terms of effect size. In the context of multiple regression, an appropriate effect size metric is Cohen f^2 that quantifies the additional variance explained by each term of the regression model.[21] According to guidance by Cohen,[22] an $f^2 > .15$ is considered a moderate effect size, whereas $f^2 > .35$ is considered to be large. The model outcome of interest for this investigation is the effect size of the term for ILAE score: the dependence of seizure outcome on regional connectivity in healthy brains to the resection zone. Our analysis sought clusters of voxels with median f^2 of at least .15, a moderate effect size, for the ILAE term. These clusters represent target regions for continued study due to the pertinence of their connectivity to TSC resection zones to seizure outcome.

A systematic, iterative thresholding process derived clusters of effect size from the voxelwise f^2 map for the ILAE term of the regression model. Starting at zero, the base f^2 threshold was increased by .001 for each iteration, after which resulting clusters of contiguous voxels (with adjacency of 18) were evaluated. Resulting clusters at each iteration were reported with median f^2 at or above the threshold of .15, with a minimum size of 10 voxels and a maximum size of 500 voxels. Clusters exceeding the f^2 threshold but smaller than 10 voxels were discarded and removed from further processing. If any clusters exceeded the median effect size threshold, but with size larger than 500 voxels, the iterative process continued within those clusters with the median effect size threshold increased by .01. Iterations of the process continued until no clusters were formed above the base f^2 threshold. We report the following for each resulting cluster: the median effect size threshold used, the peak effect size, the Montreal Neurological Institute coordinates of the peak voxel, and the anatomic localization.

3 | RESULTS

3.1 | Patients and resection ROIs

TSC patient characteristics are shown in Table 1, with details about each patient's resection region including size and lobular location. Resection ROIs for all patients are overlaid on an anatomic brain volume in Figure 1, with

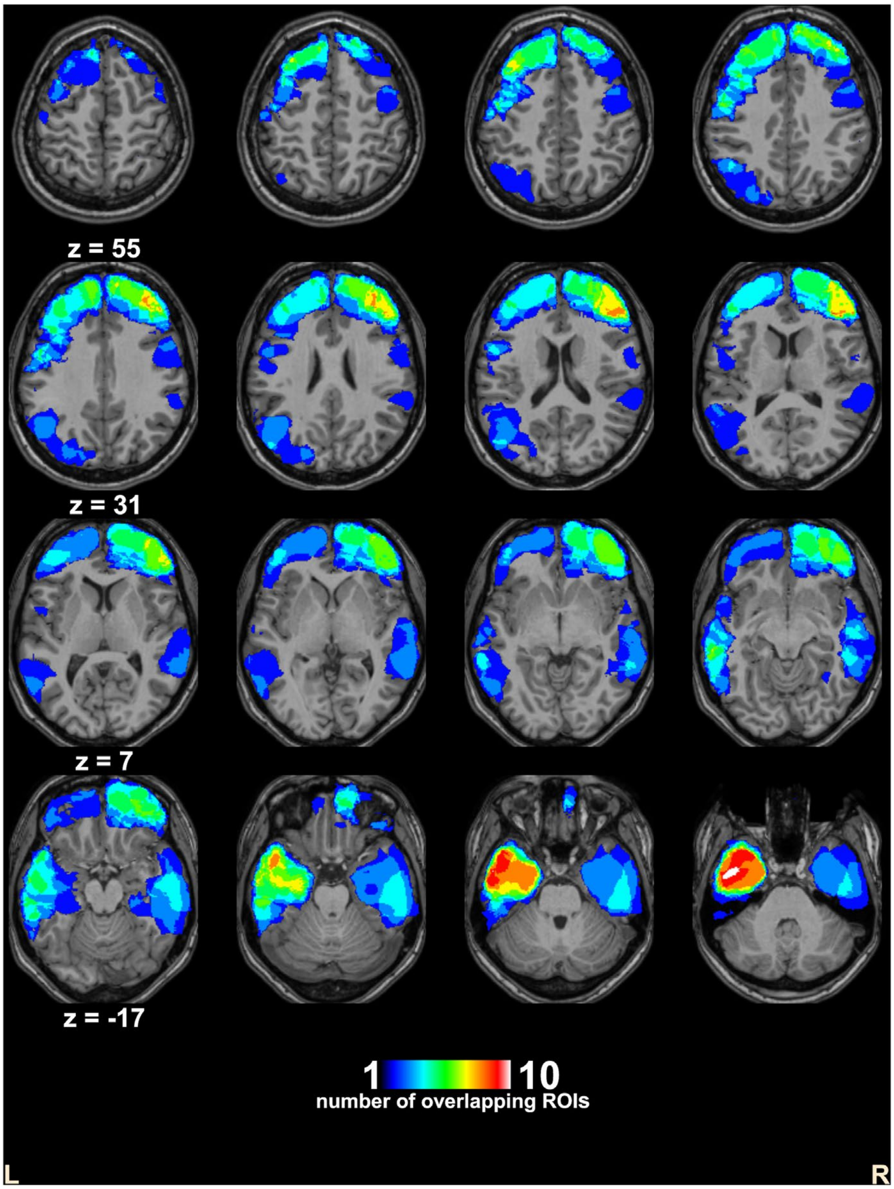

FIGURE 1 Resection region of interests (ROIs) for $n = 39$ tuberous sclerosis complex patients overlaid on a structural volume. Colors indicate the number of ROIs overlapping in each voxel according to the color bar. Montreal Neurological Institute z-coordinates are provided. Neurological orientation convention has been used (right side of brain is on right of figure). L, left; R, right.

color indicating the degree of spatial overlap. A maximum of 10 resection ROIs overlapped in the left inferior temporal region of the brain.

3.2 | Association of resection connectivity with seizure outcome

The multiple regression model term for ILAE class at follow-up had no statistically significant clusters with corrected cluster $p < .05$. Among the covariates, only age resulted in a significant cluster in the left precentral gyrus with 647 voxels and corrected $p = .04$. Effect size mapping for the ILAE class model term resulted in 17 clusters with median Cohen $f^2 > .15$, shown in Figure 2 and detailed in Table 2. The direction of dependence of cluster connectivity on seizure outcome represented by ILAE class was determined by the median coefficient value among the voxels of each cluster. Nine clusters had a positive dependence of connectivity on ILAE class, where greater connectivity to the resection zone corresponded to worse seizure outcomes at 1-year follow-up. Notably, these clusters included the bilateral insula, associative visual areas (inferior temporal and fusiform gyri), and putamen. Eight clusters represented regions with negative ILAE class coefficients, where connectivity to the resection zones was associated with better seizure outcomes. These clusters anatomically corresponded to elements of

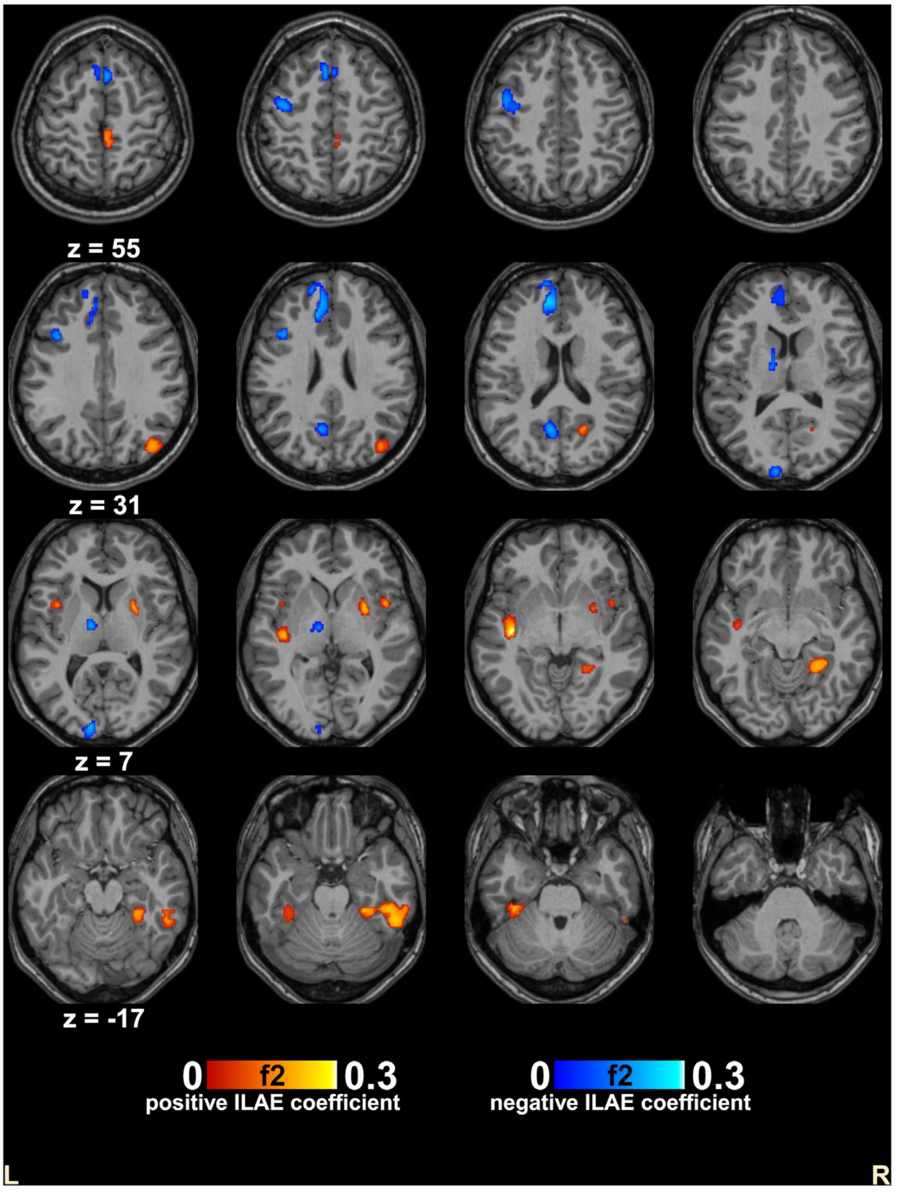

FIGURE 2 Clusters of 10–500 voxels with median Cohen f^2 of at least .15 for the International League Against Epilepsy (ILAE) class coefficient. Hot colors indicate clusters with positive ILAE coefficient. Cool colors indicate clusters with negative ILAE coefficient. Color bars represent the Cohen f^2 values. Montreal Neurological Institute z-coordinates are provided. Neurological orientation convention has been used (right side of brain is on right of figure). L, left; R, right.

the DMN (medial prefrontal cortex anteriorly and precuneus posteriorly). Areas supporting motor function were also included among the clusters with negative ILAE class dependence.

4 | DISCUSSION

4.1 | Role for further complementary tools in TSC

This study provides preliminary evidence of a relationship between brain connectivity defined by LNM in resection regions and seizure outcome. Higher connectivity to the DMN, specifically medial prefrontal and precuneus regions, or motor functional regions, was associated with better seizure outcome. This suggests that the epileptic network's response to resection of cortical tuber(s) may be predictable based on the functional networks connected to the tuber(s). Identification of the epileptic network is in itself a difficult task, because multiple cortical tubers of similar size typically exist in multiple lobes. Currently, the evaluation for epilepsy surgery relies heavily on visual analysis of iEEG recordings of habitual seizures. A majority of TSC patients who have destructive epilepsy surgery (ablation or resection) undergo invasive intracranial monitoring, with either sEEG or subdural grids and strips to plan this surgery.[23]

Seizure outcomes after surgery in TSC are highly variable, as presurgical evaluation, candidate selection factors, and surgical approach are individualized and differ greatly between centers. However, a number of pediatric retrospective studies have recently reported postoperative seizure freedom at latest follow-up of approximately 50%,[6,24] and

TABLE 2 Effect size (Cohen f^2) clusters[a] for the ILAE class coefficient.

Cluster size[b]	Median f^2 threshold	Peak f^2	Peak MNI coordinates x	y	z	Anatomic regions
Clusters with positive median ILAE class coefficient						
77	.15	.23	−34	−36	−28	Left fusiform, inf. temporal, cerebellum
488	.16	.25	41	−40	−19	Right fusiform, inf. temporal, lingual
153	.15	.36	−40	−18	−6	Left sup. temporal, insula
86	.15	.25	28	2	2	Right putamen
32	.15	.20	46	6	−2	Right insula
26	.15	.17	−38	6	6	Left insula
29	.15	.18	20	−64	18	Right calcarine, cuneus
119	.15	.20	40	−76	30	Right mid. occipital
392	.15	.32	6	−38	78	Right paracentral lobule, postcentral
Clusters with negative median ILAE class coefficient						
85	.15	.20	−10	−12	6	Left thalamus
346	.15	.25	−10	44	20	Left sup. medial frontal, ACC
103	.15	.23	−8	−62	22	Left precuneus, cuneus, calcarine
68	.15	.21	−36	16	28	Left inf. frontal
95	.15	.22	−10	−96	8	Left sup. occipital, mid. occipital
152	.15	.22	−38	−6	44	Left precentral
61	.15	.19	−4	22	50	Left SMA, sup. medial frontal
72	.15	.20	2	20	52	Bilateral SMA

Abbreviations: ACC, anterior cingulate cortex; ILAE, International League Against Epilepsy; inf., inferior; mid., middle; MNI, Montreal Neurological Institute; SMA, supplementary motor area; sup., superior.

[a]Cluster median Cohen $f^2 > .15$.

[b]Cluster size restricted to the range of 10–500 voxels.

a large review of 34 studies including 1026 patients found 48%–57% were seizure-free.[25] Children with TSC and a high seizure burden are far more likely to have autism or severe developmental delay, prompting a prospective study of neurodevelopmental outcome in early epilepsy surgery.[26]

Adoption of this multimodal approach to epilepsy surgery for this patient population appears justifiable, but candidate selection remains challenging; for example, Stomberg et al. reported that only 34 of the 85 (40%) children with TSC evaluated for epilepsy surgery underwent surgery.[7] Most of the retrospective surgical series available do not report the number of children evaluated for surgery, making it unclear how many were evaluated and how selection criteria were applied. Treiber et al. argue for a redefinition of treatment goals that incorporates seizure reduction and quality of life, rather than a seizure-free absolutism approach.[16] Therefore, the problem may be twofold: (1) lack of consensus regarding optimal surgical candidates and (2) incomplete prediction of outcomes using current tools.

Preoperative predictors of poor outcome in epilepsy surgery for patients with TSC are not well established but include high number of cortical tubers (≥5) and seizure onset before 1 year of age,[6] with mixed results relating to whether complete removal of the SOZ is necessary for seizure freedom.[27,28] Previously, we found that more limited extent and number of SOZs, as identified by iEEG, were predictive of seizure freedom following epilepsy surgery in pediatric TSC patients.[29] This suggests that invasive EEG can be used as a surrogate to determine whether the epileptogenic zone is narrowly focused, favoring improved postoperative outcome.

4.2 | Resting state and structural connectivity in epilepsy surgery and TSC

Even a single FCD lesion has measurable effects on connectivity networks. Using an assessment of fMRI based on independent component analysis, Liu et al. found higher connectivity in the DMN, dorsal attention network, and sensorimotor mode network compared to controls.[30] The effects of heterogeneous or multiple lesions on networks are now being studied and applied to surgical planning. rs-fMRI has been used to conserve eloquent tissue for patients undergoing resective or ablative surgery for TSC, brain tumors,[31,32] and epilepsy.[33,34] Lobanov et al. found that a majority of TSC patients had similar connectivity network architecture when compared to healthy controls, but aberrant differences in connectivity within the TSC cohort, particularly in the cingulo-opercular and visual resting-state networks, correlated with higher tuber burden and poorer neurodevelopmental state.[35] Akhondi-Asl et al. detected a significant difference in global functional connectivity between TSC patients and healthy controls using rs-fMRI analysis.[36] Im et al., using diffusion tensor imaging to assess structural connectivity between brain regions by axonal fibers in white matter, found that both short- and long-association fibers were reduced in TSC patients, with interhemispheric connectivity being particularly diminished; findings also reflected a correlation between altered structural connectivity in TSC patients and tuber burden.[37] Similarly, rs-fMRI has been used to correlate network connectivity with neurodevelopmental outcomes, autism, and seizure history in infants with TSC.[38]

4.3 | Use of LNM in epilepsy and TSC

LNM is a tool that may supplement evaluation of a given brain region and epilepsy risk, even if a functional connectome cannot be obtained for a given patient due to difficulty with development or participation. For this reason, in our estimation, LNM has a wider potential for clinical application in TSC compared to rs-fMRI. By employing lesions as seeds and mapping these seeds to corresponding brain connectomes from healthy participants, it is possible to determine which networks "ought" to be connected to these brain regions. Schaper et al.[39] reported the use of LNM to stratify epilepsy risk after stroke and found that functional connectivity to the basal ganglia and cerebellum increased in this LNM. Because there are multiple lesions that are often confluent in certain regions, there may be a cumulative effect on brain networks. Furthermore, TSC is a developmental epilepsy, meaning that the epileptic network develops alongside functional networks as the child grows. This can result in altered white matter (measurable using diffusion tensor imaging) that results in neurobehavioral abnormalities, autism, and intellectual disability.[40] Therefore, the underlying brain networks in TSC may be distorted or shifted compared to healthy controls.

Despite the challenges of applying LNM to TSC, this approach has been applied successfully to another commonly seen brain phenotype in this population. TSC patients with infantile spasms were more likely to have tubers "negatively connected" to the globi pallidi and cerebellar vermis.[41] In this study, the authors corrected for overall tuber burden and location as well as TSC genotype (*TSC1* vs. *TSC2*), because both higher tuber burden and *TSC2* genotype are associated with infantile spasm development. The pathophysiological implications of this finding are speculative, but the authors concluded that "lesion network mapping of individual tuber lesions rather than lesion patterns…" may identify tuber candidates for destructive surgery.

4.4 | Comparison to our previous work in FCD

The potential value of LNM for predicting efficacy of destructive surgery was explored in our previous publication.[13] In this work, we identified 21 pediatric patients who underwent resective surgery for epilepsy secondary to FCD (without TSC genotype/phenotype). The voxel-based seeds were defined by the MRI-visible lesions, and connectivity was compared between seizure-free and persistent seizure groups. The majority (19/21) had complete resection of these lesions. The resulting LNM identified weaker connectivity to the DMN in those with persistent seizures after surgery compared to the seizure-free group, a finding that aligns with the current study.

4.5 | Potential role of DMN

The role of the DMN, specifically, in epilepsy is complex. Patients with temporal lobe seizures have reduced blood flow in the DMN during seizures that involves alteration of consciousness.[42] Additionally, epilepsy patients may have decreased functional connectivity within the DMN interictally compared to controls, and the degree of decreased connectivity may predict seizure freedom after temporal lobe surgery.[43] However, the status of the DMN in pediatric extratemporal epilepsies is unclear; a study of patients with benign epilepsy with centrotemporal spikes demonstrated increased variability of functional connectivity in the precuneus compared to controls.[44] In the current study, resection of regions connected to motor networks and DMNs was associated with improved outcome. We can postulate that disabling seizure networks that participate in core functions that include consciousness or movement would be desirable. This does not explain why tubers connected to these regions are more intervenable with surgery, although these seizures may be the most obvious to caregivers.

4.6 | Limitations

There are several major differences in study population between isolated FCD, analyzed in our previous work, and the TSC population, resulting in a more nuanced analysis pipeline. Foremost, the volume of brain resected was larger in the current study and frequently multilobar. Factors affecting resection volume included surgical–anatomical boundaries and presence of multiple tubers in the SOZ(s). Patients with TSC are more likely to have multiple SOZs and seizure types. Considering this large resection volume as a "lesion" leads to the increased possibility of making a type II error. Consequently, the analysis in the current work used the first principal component of the ROI (overall resection volume), anticipating that this would narrow the connectomes being compared. Clusters with negative coefficients were predominantly located in the left hemisphere. It is possible that this laterality is a consequence of the considerable overlap of resection ROI in left temporal regions among patients in our cohort. Future LNM studies would benefit from larger cohorts with wider variation in ROI distribution. Other limitations include a moderate effect size and variable antiepileptic drug regimens including presence/absence of mTOR inhibitor use.

4.7 | Conclusions

We provide methods for application of an LNM technique to assess the relationship between functional connectivity and epilepsy surgery outcomes in pediatric TSC. Our findings corroborate a previous study, identifying the potential role of the DMN. Patients with resected lesions in brain regions connected to the DMN had better postoperative seizure outcomes. Further development of LNM methods for TSC patients may provide ancillary support for treatment decision-making.

AUTHOR CONTRIBUTIONS

Kara B. Miecznikowski: Conceptualization (supporting); data curation (lead); formal analysis (supporting); investigation (equal); software (supporting); writing—original draft preparation (equal). **Hansel M. Greiner**: Conceptualization (lead); investigation (equal); methodology (supporting); project administration (lead); writing—original draft preparation (equal); supervision (lead). **James Leach**: Visualization (supporting); writing—review & editing (equal). **Leonid Rozhkov**: Visualization (supporting); writing—review & editing (equal). **Francesco T. Mangano**: Writing—review & editing (equal). **Darcy A. Krueger**: Writing—review & editing (equal). **Mark W. DiFrancesco**: Methodology (lead); software (lead); formal analysis (lead); investigation (equal); writing—original draft preparation (equal); visualization (lead).

ACKNOWLEDGMENTS

There are no funding sources to report for this study.

CONFLICT OF INTEREST STATEMENT

None of the authors has any conflict of interest to disclose.

DATA AVAILABILITY STATEMENT

The data that support the findings of this study are available from the corresponding author upon reasonable request.

ETHICAL PUBLICATION STATEMENT

We confirm that we have read the Journal's position on issues involved in ethical publication and affirm that this report is consistent with those guidelines. This study was performed in accordance with the ethical standards in the 1964 Declaration of Helsinki. This study was carried out in accordance with relevant regulations of the US Health Insurance Portability and Accountability Act. Details that might disclose the identity of the subjects under study have been omitted. This study was approved by the institutional review board (ID: 2021-0802).

ORCID

Kara B. Miecznikowski https://orcid.org/0000-0001-8826-0613
Hansel M. Greiner https://orcid.org/0000-0001-7479-1384
Mark W. DiFrancesco https://orcid.org/0000-0001-8002-0332

REFERENCES

1. Curatolo P, Bombardieri R, Jozwiak S. Tuberous sclerosis. Lancet. 2008;372(9639):657–68. https://doi.org/10.1016/S0140-6736(08)61279-9
2. Curatolo P, Bombardieri R. Tuberous sclerosis. Handbook of clinical neurology. Volume 87. Amsterdam, Netherlands: Elsevier; 2007. p. 129–51. https://doi.org/10.1016/S0072-9752(07)87009-6
3. Mühlebner A, van Scheppingen J, Hulshof HM, Scholl T, Iyer AM, Anink JJ, et al. Novel histopathological patterns in cortical tubers of epilepsy surgery patients with tuberous sclerosis complex. PLoS One. 2016;11(6):e0157396. https://doi.org/10.1371/journal.pone.0157396
4. Teutonico F, Mai R, Devinsky O, Lo Russo G, Weiner HL, Borrelli P, et al. Epilepsy surgery in tuberous sclerosis complex: early predictive elements and outcome. Childs Nerv

Syst. 2008;24(12):1437–45. https://doi.org/10.1007/s00381-008-0679-4
5. Jansen FE, Van Huffelen AC, Algra A, Van Nieuwenhuizen O. Epilepsy surgery in tuberous sclerosis: a systematic review: Epilepsy surgery in tuberous sclerosis. Epilepsia. 2007;48(8):1477–84. https://doi.org/10.1111/j.1528-1167.2007.01117.x
6. Vannicola C, Tassi L, Barba C, Boniver C, Cossu M, de Curtis M, et al. Seizure outcome after epilepsy surgery in tuberous sclerosis complex: results and analysis of predictors from a multicenter study. J Neurol Sci. 2021;427:117506. https://doi.org/10.1016/j.jns.2021.117506
7. Stomberg M, Bien CG, Kalbhenn T, Polster T, May TW. Epilepsy associated with tuberous sclerosis complex in childhood: long-term outcome in children after epilepsy surgery and children non-eligible for epilepsy surgery. Epilepsy Behav. 2021;122:108210. https://doi.org/10.1016/j.yebeh.2021.108210
8. Liang S, Zhang J, Yang Z, Zhang S, Cui Z, Cui J, et al. Long-term outcomes of epilepsy surgery in tuberous sclerosis complex. J Neurol. 2017;264(6):1146–54. https://doi.org/10.1007/s00415-017-8507-y
9. Buxton RB, Uludağ K, Dubowitz DJ, Liu TT. Modeling the hemodynamic response to brain activation. Neuroimage. 2004;23:S220–S233. https://doi.org/10.1016/j.neuroimage.2004.07.013
10. Lv H, Wang Z, Tong E, Zaharchuk G, Zeineh M, Goldstein-Piekarski AN, et al. Resting-state functional MRI: everything that nonexperts have always wanted to know. Am J Neuroradiol. 2018;39(8):1390–9. https://doi.org/10.3174/ajnr.A5527
11. Lee MH, Smyser CD, Shimony JS. Resting-state fMRI: a review of methods and clinical applications. Am J Neuroradiol. 2013;34(10):1866–72. https://doi.org/10.3174/ajnr.A3263
12. Zhang D, Raichle ME. Disease and the brain's dark energy. Nat Rev Neurol. 2010;6(1):15–28. https://doi.org/10.1038/nrneurol.2009.198
13. Bdaiwi AS, Greiner HM, Leach J, Mangano FT, DiFrancesco MW. Categorizing cortical dysplasia lesions for surgical outcome using network functional connectivity. J Neurosurg Pediatr. 2021;28(5):600–8. https://doi.org/10.3171/2021.5.PEDS20990
14. Thomas Yeo BT, Krienen FM, Sepulcre J, Sabuncu MR, Lashkari D, Hollinshead M, et al. The organization of the human cerebral cortex estimated by intrinsic functional connectivity. J Neurophysiol. 2011;106(3):1125–65. https://doi.org/10.1152/jn.00338.2011
15. Mithani K, Boutet A, Germann J, Elias GJB, Weil AG, Shah A, et al. Lesion network localization of seizure freedom following MR-guided laser interstitial thermal ablation. Sci Rep. 2019;9(1):18598. https://doi.org/10.1038/s41598-019-55015-y
16. Treiber JM, Curry DJ, Weiner HL, Roth J. Epilepsy surgery in tuberous sclerosis complex (TSC): emerging techniques and redefinition of treatment goals. Childs Nerv Syst. 2020;36(10):2519–25. https://doi.org/10.1007/s00381-020-04715-2
17. Commission on Neurosurgery of the International League Against Epilepsy (ILAE) 1997–2001, Wieser HG, Blume WT, Fish D, Goldensohn E, Hufnagel A, et al. Proposal for a new classification of outcome with respect to epileptic seizures following epilepsy surgery. Epilepsia. 2008;42(2):282–6. https://doi.org/10.1046/j.1528-1157.2001.35100.x
18. Vannest J, Rajagopal A, Cicchino N, Franks-Henry J, Simpson S, Lee G, et al. Factors determining success of awake and asleep magnetic resonance imaging scans in nonsedated children. Neuropediatrics. 2014;45(06):370–7. https://doi.org/10.1055/s-0034-1387816
19. Ashburner J, Friston KJ. Unified segmentation. Neuroimage. 2005;26(3):839–51. https://doi.org/10.1016/j.neuroimage.2005.02.018
20. Whitfield-Gabrieli S, Nieto-Castanon A. Conn: a functional connectivity toolbox for correlated and Anticorrelated brain networks. Brain Connect. 2012;2(3):125–41. https://doi.org/10.1089/brain.2012.0073
21. Selya AS, Rose JS, Dierker LC, Hedeker D, Mermelstein RJ. A practical guide to calculating Cohen's f2, a measure of local effect size, from PROC MIXED. Front Psychol. 2012;3:111. https://doi.org/10.3389/fpsyg.2012.00111
22. Cohen J. Statistical power analysis for the behavioral sciences. London: Routledge; 2013. https://doi.org/10.4324/9780203771587
23. Ravindra VM, Karas PJ, Lazaro TT, Coorg R, Awad AW, Patino I, et al. Epilepsy surgery in young children with tuberous sclerosis complex: a novel hybrid multimodal surgical approach. Neurosurgery. 2023;92(2):398–406. https://doi.org/10.1227/neu.0000000000002214
24. Liu S, Yu T, Guan Y, Zhang K, Ding P, Chen L, et al. Resective epilepsy surgery in tuberous sclerosis complex: a nationwide multicentre retrospective study from China. Brain. 2020;143(2):570–81. https://doi.org/10.1093/brain/awz411
25. Specchio N, Pepi C, De Palma L, Moavero R, De Benedictis A, Marras CE, et al. Surgery for drug-resistant tuberous sclerosis complex-associated epilepsy: who, when, and what. Epileptic Disord. 2021;23(1):53–73. https://doi.org/10.1684/epd.2021.1253
26. Grayson LE, Peters JM, McPherson T, Krueger DA, Sahin M, Wu JY, et al. Pilot study of neurodevelopmental impact of early epilepsy surgery in tuberous sclerosis complex. Pediatr Neurol. 2020;109:39–46. https://doi.org/10.1016/j.pediatrneurol.2020.04.002
27. Fujiwara H, Greiner HM, Lee KH, Holland-Bouley KD, Seo JH, Arthur T, et al. Resection of ictal high-frequency oscillations leads to favorable surgical outcome in pediatric epilepsy: HFO in ICEEG and surgical outcome. Epilepsia. 2012;53(9):1607–17. https://doi.org/10.1111/j.1528-1167.2012.03629.x
28. Huang C, Marsh E, Ziskind D, Celix J, Peltzer B, Brown M, et al. Leaving tissue associated with infrequent intracranial EEG seizure onsets is compatible with post-operative seizure freedom. J Pediatr Epilepsy. 2015;01(04):211–9. https://doi.org/10.3233/PEP-12033
29. Miecznikowski KB, Leach J, Rozhkov L, Mangano FT, Skoch J, Krueger DA, et al. Impact of seizure onset zone and intracranial electroencephalography ictal characteristics on epilepsy surgery outcomes in tuberous sclerosis complex. Epilepsy Res. 2024;205:107422. https://doi.org/10.1016/j.eplepsyres.2024.107422
30. Liu W, Lin M, Yue Q, Gong Q, Zhou D, Wu X. Brain functional connectivity patterns in focal cortical dysplasia related epilepsy. Seizure. 2021;87:1–6. https://doi.org/10.1016/j.seizure.2021.02.009
31. Zhang D, Johnston JM, Fox MD, Leuthardt EC, Grubb RL, Chicoine MR, et al. Preoperative sensorimotor mapping in brain tumor patients using spontaneous fluctuations in neuronal

activity imaged with functional magnetic resonance imaging: initial experience. Oper Neurosurg. 2009;65(6):ons226–ns236. https://doi.org/10.1227/01.NEU.0000350868.95634.CA

32. Kokkonen SM, Nikkinen J, Remes J, Kantola J, Starck T, Haapea M, et al. Preoperative localization of the sensorimotor area using independent component analysis of resting-state fMRI. Magn Reson Imaging. 2009;27(6):733–40. https://doi.org/10.1016/j.mri.2008.11.002
33. Liu H, Buckner RL, Talukdar T, Tanaka N, Madsen JR, Stufflebeam SM. Task-free presurgical mapping using functional magnetic resonance imaging intrinsic activity: laboratory investigation. J Neurosurg. 2009;111(4):746–54. https://doi.org/10.3171/2008.10.JNS08846
34. Pur DR, Eagleson R, Lo M, Jurkiewicz MT, Andrade A, De Ribaupierre S. Presurgical brain mapping of the language network in pediatric patients with epilepsy using resting-state fMRI. J Neurosurg Pediatr. 2021;27(3):259–68. https://doi.org/10.3171/2020.8.PEDS20517
35. Lobanov OV, Shimony JS, Kenley J, Kaplan S, Alexopoulos D, Roland JL, et al. Alterations in resting-state functional connectivity in pediatric patients with tuberous sclerosis complex. Epilepsia Open. 2021;6(3):579–87. https://doi.org/10.1002/epi4.12523
36. Akhondi-Asl A, Hans A, Scherrer B, Peters JM, Warfield SK. Whole brain group network analysis using network bias and variance parameters. 2012 9th IEEE international symposium on biomedical imaging (ISBI). Piscataway, NJ: IEEE; 2012. p. 1511–4. https://doi.org/10.1109/ISBI.2012.6235859
37. Im K, Ahtam B, Haehn D, Peters JM, Warfield SK, Sahin M, et al. Altered structural brain networks in tuberous sclerosis complex. Cereb Cortex. 2016;26(5):2046–58. https://doi.org/10.1093/cercor/bhv026
38. Ahtam B, Dehaes M, Sliva DD, Peters JM, Krueger DA, Bebin EM, et al. Resting-state fMRI networks in children with tuberous sclerosis complex. J Neuroimaging. 2019;29(6):750–9. https://doi.org/10.1111/jon.12653
39. Schaper, FLWVJ, Nordberg, J, Cohen, AL, Lin, C, Hsu, J, Horn, A, et al. Mapping Lesion-Related Epilepsy to a Human Brain Network. JAMA Neurology2023;80(9):891. https://doi.org/10.1001/jamaneurol.2023.1988.
40. Tsai JD, Ho MC, Lee HY, Shen CY, Li JY, Weng JC. Disrupted white matter connectivity and organization of brain structural connectomes in tuberous sclerosis complex patients with neuropsychiatric disorders using diffusion tensor imaging. Magn Reson Mater Phys Biol Med. 2021;34(2):189–200. https://doi.org/10.1007/s10334-020-00870-4
41. Cohen AL, Mulder BPF, Prohl AK, Soussand L, Davis P, Kroeck MR, et al. Tuber locations associated with infantile spasms map to a common brain network. Ann Neurol. 2021;89(4):726–39. https://doi.org/10.1002/ana.26015
42. Blumenfeld H, McNally KA, Vanderhill SD, Paige AL, Chung R, Davis K, et al. Positive and negative network correlations in temporal lobe epilepsy. Cereb Cortex. 2004;14(8):892–902. https://doi.org/10.1093/cercor/bhh048
43. Ofer I, LeRose C, Mast H, LeVan P, Metternich B, Egger K, et al. Association between seizure freedom and default mode network reorganization in patients with unilateral temporal lobe epilepsy. Epilepsy Behav. 2019;90:238–46. https://doi.org/10.1016/j.yebeh.2018.10.025
44. Li R, Wang L, Chen H, Guo X, Liao W, Tang YL, et al. Abnormal dynamics of functional connectivity density in children with benign epilepsy with centrotemporal spikes. Brain Imaging Behav. 2019;13(4):985–94. https://doi.org/10.1007/s11682-018-9914-0

How to cite this article: Miecznikowski KB, Greiner HM, Leach J, Rozhkov L, Mangano FT, Krueger DA, et al. Prognostic application of lesion network mapping to epilepsy surgery outcomes in pediatric tuberous sclerosis complex. Epilepsia. 2025;66:1854–1864. https://doi.org/10.1111/epi.18320